ORIGINAL RESEARCH

Secretory Inositol Polyphosphate 4-Phosphatase Protects against Airway Inflammation and Remodeling

Kritika Khanna[1,2,3]*, Rituparna Chaudhuri[1,2,3]*, Jyotirmoi Aich[1], Bijay Pattnaik[1,2,4], Lipsa Panda[1,2,3], Y. S. Prakash[5,6,7], Ulaganathan Mabalirajan[1,2], Balaram Ghosh[1,2,3], and Anurag Agrawal[1,2,3]

[1]Centre of Excellence for Translational Research in Asthma and Lung Disease, [2]Molecular Immunogenetics Laboratory, and [3]Academy of Scientific and Innovative Research, CSIR-Institute of Genomics and Integrative Biology, Delhi, India; [4]Department of Pulmonary Medicine and Sleep Disorders, All India Institute of Medical Sciences, New Delhi, India; and [5]Department of Anesthesiology, [6]Department of Physiology, and [7]Department of Biomedical Engineering, Mayo Clinic, Rochester, Minnesota

ORCID IDs: 0000-0003-0463-8442 (K.K.); 0000-0002-2547-1023 (U.M.); 0000-0002-0340-5252 (A.A.).

Abstract

The asthma candidate gene inositol polyphosphate 4-phosphatase type I A (*INPP4A*) is a lipid phosphatase that negatively regulates the PI3K/Akt pathway. Destabilizing genetic variants of *INPP4A* increase the risk of asthma, and lung-specific INPP4A knockdown induces asthma-like features. INPP4A is known to localize intracellularly, and its extracellular presence has not been reported yet. Here we show for the first time that INPP4A is secreted by airway epithelial cells and that extracellular INPP4A critically inhibits airway inflammation and remodeling. INPP4A was present in blood and BAL fluid, and this extracellular INPP4A was reduced in patients with asthma and mice with allergic airway inflammation. In both naive mice and mice with allergic airway inflammation, antibody-mediated neutralization of extracellular INPP4A potentiated PI3K/Akt signaling and induced airway hyperresponsiveness, with prominent airway remodeling, subepithelial fibroblast proliferation, and collagen deposition. The link between extracellular INPP4A and fibroblasts was investigated *in vitro*. Cultured airway epithelial cells secreted enzymatically active INPP4A in extracellular vesicles and in a free form. Extracellular vesicle–mediated transfer of labeled INPP4A, from epithelial cells to fibroblasts, was observed. Inhibition of such transfer by anti-INPP4A antibody increased fibroblast proliferation. We propose that secretory INPP4A is a novel "paracrine" layer of the intricate regulation of lung homeostasis, by which airway epithelium dampens PI3K/Akt signaling in inflammatory cells or local fibroblasts, thereby limiting inflammation and remodeling.

Keywords: airway remodeling asthma; exosomes; INPP4A; microvesicles; PI3K/Akt signaling

Clinical Relevance

We identify secretion of INPP4A, an important regulator of the PI3K pathway, by airway epithelium via exosomes. Extracellular INPP4A attenuates airway inflammation and remodeling. This provides a new therapeutic strategy for inhibiting lung remodeling during epithelial injury.

Inositol polyphosphate 4-phosphate, type 1 (INPP4A) is a lipid phosphatase that dephosphorylates phosphatidyl inositol (3,4)-bisphosphate ($PI(3,4)P_2$) to phosphatidyl inositol 3-phosphate (PI(3)P) (1). By modulating phosphoinositide levels at the cell membrane, INPP4A acts as an important negative regulator of the PI3K signaling pathway (2–4). *INPP4A* was previously reported to be genetically associated with asthma, with a genetic polymorphism that makes it prone to degradation and renders individuals susceptible to the disease (5). Functional studies in a murine model of allergic airway inflammation (AAI) have demonstrated that INPP4A is richly expressed in airway epithelial cells, and inhaled siRNA-mediated knockdown of INPP4A worsens the asthma phenotype (6). Interestingly, loss of INPP4A in a naive murine model was associated with spontaneous development of airway hyperresponsiveness (AHR), indicating that INPP4A could be vital for lung homeostasis (6). Additionally, INPP4A has been implicated in regulating cell proliferation and apoptosis (4, 7, 8). It has also been reported to localize to early and recycling endosomes to modulate vesicular trafficking by regulating phosphoinositide levels at these vesicles (9, 10). However, all the effects of INPP4A reported so far are exerted through its actions within the boundaries of the cell. Its presence and functional role outside of the cellular space have not yet been reported.

Various proteins act both intracellularly and extracellularly, with their secretory versions mediating intercellular communication and thereby orchestrating changes on a broader (tissue-level) scale. Extracellular secretion of proteins can occur via two pathways: the classical secretory pathway and the nonclassical secretory pathway. Proteins with a signal peptide enter the classical endoplasmic reticulum–Golgi pathway to get secreted out of the cell (11, 12). However, numerous proteins can be secreted even without any signal peptide, via unconventional mechanisms (13–15). Proteins that take such unconventional paths can translocate directly through the membrane and be released from the cells (16, 17) or they can use organelles such as endosomes, autophagosomes, and secretory lysosomes for secretion (14). Among the various mechanisms of unconventional protein secretion, organelle-mediated secretion via

extracellular vesicles (EVs; namely, exosomes and microvesicles) (18), is the best studied. These EVs can carry protein, RNA, microRNA, and lipids, and thereby mediate cell–cell communication (18–20). Exosomes are vesicles that are derived from endosomes and range in size from 50 to 100 nm. Inward endosomal budding leads to the formation of multivesicular bodies, and the fusion of such a multivesicular body with the plasma membrane leads to the release of intraluminal vesicles, called exosomes. Microvesicles, on the other hand, are larger vesicles (0.1–1 μm in size) that directly bud off from the plasma membrane. Many reports have described EVs as important mediators of intercellular communication in the lung, under both homeostatic conditions and stress physiology (21–25). In the lung, the epithelium has been shown to be one of the major secretors of EVs (24), and to thus mediate critical crosstalk with the mesenchymal unit (26, 27). Because the lung epithelium is the first line of defense, any detrimental exposure to external agents such as aero-allergens, air pollutants, and pathogens can modulate its secretions and perturb the lung homeostasis.

INPP4A has been reported to localize to endosomes (9, 10), and this compartment is involved in exosome-mediated unconventional secretion of proteins. In the current study, we report for the first time that extracellular secretion of INPP4A by airway epithelial cells critically inhibits airway inflammation and remodeling.

Methods

Clinical Material
Human lung specimens were obtained from patients undergoing thoracic surgery at the Mayo Clinic, after approval from the institutional review board ($n = 6$ normal subjects, $n = 7$ patients with asthma). Serum ($n = 22$ normal subjects, $n = 27$ patients with asthma) and BAL fluid (BALF) samples ($n = 3$ normal and $n = 3$ patients with asthma) were obtained from atopic patients with asthma and healthy subjects recruited for our earlier studies (5). Details regarding the selected individuals are provided in the data supplement and Table 1.

Mice
BALB/c mice (6–8 weeks old) were maintained at the CSIR-Institute of

Genomics and Integrative Biology, Delhi, India. All protocols were approved by the institutional animal ethics committee. The mouse groups are described in detail in the data supplement.

Sensitization and Challenge of Mice
Immunization and challenge of mice were performed as described previously (6). Briefly, mice were sensitized with three intraperitoneal injections of 50 μg ovalbumin (OVA, chicken egg ovalbumin, grade V, Sigma Chemical Co.) with 4 mg alum (OVA mice group) or only 4 mg alum (sham mice) on Days 0, 7, and 14 of the model. After 1 week, the mice were challenged with 3% aerosolized OVA (OVA group) or PBS (sham group) for 7 consecutive days, for a duration of 30 minutes each day, using a nebulizer (flow rate: 9 L·min^{-1}; OMRON CX3 model) (*see* Figure 3A).

Antibody-mediated Neutralization of Extracellular INPP4A *In Vivo*
To carry out neutralization of secretory INPP4A in mice, anti-INPP4A antibody was used, with isotype antibody as a control (both from Santa Cruz Biotechnology). In the murine model of AAI, the anti-INPP4A antibody (2.5 mg·kg^{-1} body weight) and isotype antibody (2.5 mg·kg^{-1} body weight) were given intraperitoneally in a 200 μl volume per dose once on Days 25, 26, and 27 of the OVA challenge (*see* Figure 3A). For the naive model, three intraperitoneal injections of antibody (2.5 mg·kg^{-1} body weight anti-INPP4A or isotype antibody) were given to the mice on Days 1, 3, and 5 of the model, after which total airway resistance (AHR) measurements were obtained and the mice were killed (*see* Figure 2A).

AHR
AHR was measured using the flexiVent (Scireq) invasive airway mechanics system as described previously (6) and detailed in the data supplement.

Lung Histopathology
Lung sections were stained with hematoxylin and eosin, periodic acid–Schiff, or Masson's trichrome as described previously. Quantitative analysis of peribronchial and perivascular inflammation was also done as described previously (6) and detailed in the data supplement.

Table 1. Age and Sex Distribution of Subjects with and without Asthma

		Number of Subjects		
		Males	Females	Age (Mean ± SEM)
Lung samples	Without asthma	2	4	59.5 ± 6.026
	With asthma	1	6	51.71 ± 6.92
Sera and BAL fluid samples	Without asthma	12	11	30.3 ± 2.678
	With asthma	15	12	29.48 ± 3.357

INPP4 Activity Measurement

INPP4 activity was estimated via a competitive ELISA (Echelon Biosciences) according to the manufacturer's protocol with slight modifications as detailed in the data supplement.

ELISA

Levels of INPP4A were measured in BALF and sera using ELISA (Cloud-Clone Corp.) according to the manufacturer's protocol. In BALF, the INPP4A levels were normalized to the amount of total protein in the sample. Levels of mediators of the PI3K pathway (phosphorylated Akt [pAkt], phosphoinositide-dependent kinase-1 [PDK1], and Akt kinase activity), various cytokines (IL-4, IL-5, and IL-13), and OVA-specific IgG were measured by ELISA as described previously (6).

Immunohistochemistry

Immunohistochemistry was performed using anti–α-smooth muscle actin (α-SMA) antibody (Abcam) and anti–Ki-67 antibody (Abcam), with horseradish peroxidase–conjugated secondary antibodies (Banglore Genei). Details regarding the immunohistochemistry and immunofluorescence are provided in the data supplement.

Collagen Content Measurement

The amount of collagen in the total lung lysates was measured with a Sircol assay kit (Biocolor, Carrickfergus) according to the manufacturer's protocol.

Cell Line

Human transformed bronchial epithelial cells (BEAS-2B), human normal lung fibroblast cells (MRC-5 and HFL), and human breast adenocarcinoma cells (MCF-7) were obtained from ATCC. Primary normal human bronchial epithelial cells were obtained from Lonza. Primary normal

human lung fibroblasts were isolated at the Mayo Clinic as described elsewhere (28). A detailed description of the culture methods is provided in the data supplement.

Conditioned Media Processing and Exosome Isolation

Two methods were used for conditioned media processing from the cells: trichloroacetic acid–based precipitation and 100 kD cutoff filters, as detailed in the data supplement. To compare the secretion of INPP4A in conditioned media of epithelial cells and fibroblasts, equal numbers of cells were seeded for each cell type in the same volume of culture media. This was followed by concentrating the conditioned media to the same volume using 100 kD cutoff filters. Because the cell types used in the experiment were different and had variable secretory profiles, loading equal protein would not have been ideal, as a variable abundance of other proteins could have skewed the loading amount and thus detection of our desired protein, i.e., INPP4A.

Exosomes were isolated using differential ultracentrifugation as described in detail in the data supplement.

Immunocytochemistry and Immunoblotting

Details regarding the immunocytochemistry and Western blot analysis are provided in the data supplement.

Proliferation Assay Using Flow Cytometry

Proliferation of MRC-5 cells was assessed using a carboxyfluorescein diacetate succinimidyl ester (CFSE) dye dilution assay as detailed in the data supplement.

Statistical analyses. Statistical analyses were performed using GraphPad Prism software. Data are presented as mean ± SEM. ANOVA was used to compare more than two groups, followed by Tukey's *post*

hoc analysis. Between two groups, an unpaired Student's *t* test was used. Statistical significance was set at $P \leqslant 0.05$. For further details, see the data supplement.

Results

Reduction of Extracellular INPP4A in Asthma

To determine whether INPP4A is present extracellularly, we measured the levels of INPP4A in relevant human and mouse samples. The age and sex distribution of the human subjects is shown in **Table 1**. Consistent with prior data from experimental models of asthma in mice, INPP4A protein was reduced in the lung lysates of human patients with asthma compared with normal subjects (Figures 1A and 1B). Importantly, INPP4A was clearly present in human and mouse BAL fluid (BALF) (Figures 1C and 1E) and in human sera (Figure 1D) with the same pattern (i.e., reduced in samples from subjects with asthma compared with normal subjects).

Antibody-mediated Neutralization of Extracellular INPP4A in Naive Mice Leads to Induction of an Asthma-Like Phenotype

To determine whether extracellular INPP4A is functionally relevant, we performed antibody-mediated neutralization of extracellular INPP4A in naive mice (Figure 2A). A reduction in INPP4A activity (measured by the amount of PI(3)P produced, normalized to the total protein) in BALF revealed an efficient neutralization of extracellular INPP4A (Figure E1A). Even without any allergen sensitization and challenge, we observed a significant increase in AHR upon treatment with anti-INPP4A antibody as compared with the isotype antibody control (Figure 2B). Interestingly, there was an inverse correlation of the INPP4 activity in BALF with AHR (Figure 2C). The histological studies revealed that there was an increase in inflammatory cell infiltrates (Figure 2D; quantified in Figure E1B). Although we observed an increase in the total cell count in the BALF (Figure E1C), no significant change was observed in the differential cell counts, barring a slight trend toward an increase in neutrophils upon anti-INPP4A antibody treatment (Figure E1D). Also, there was no increase in the mucin content (Figure 2E) in the lungs of mice treated
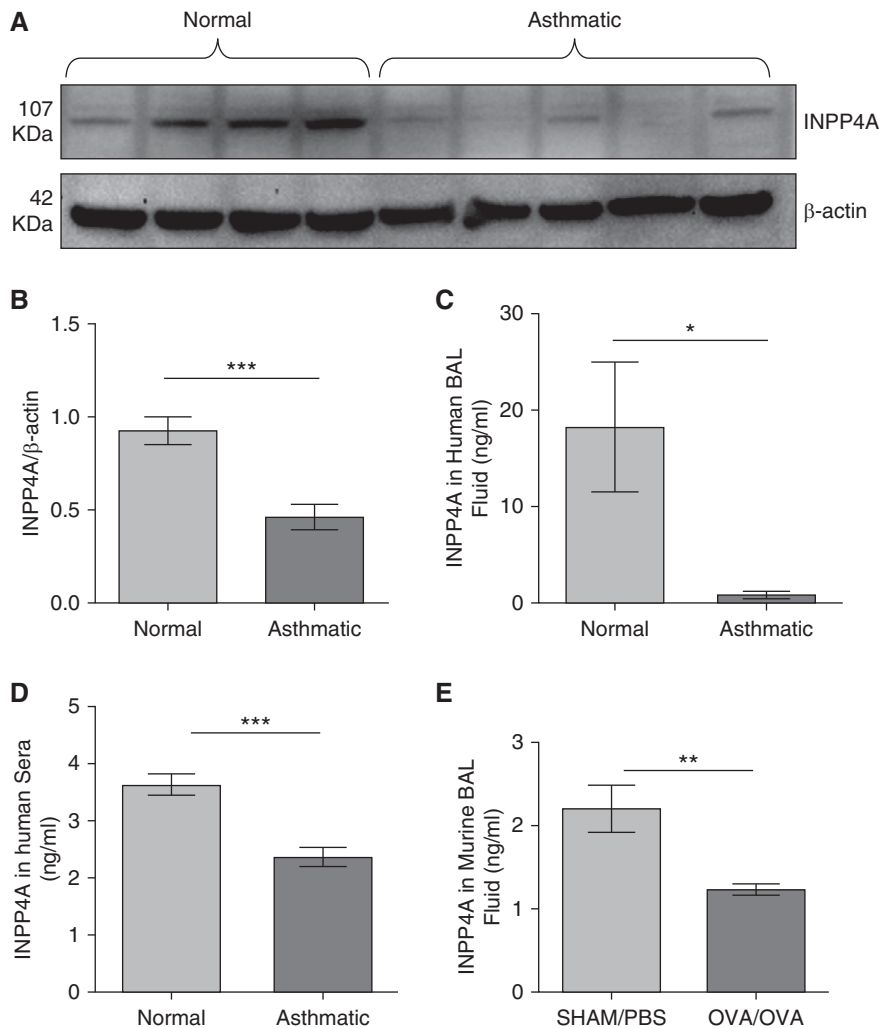
Figure 1. Loss of inositol polyphosphate-4-phosphatase type I A (INPP4A) in the lungs and physiological fluids of allergic mice and human patients with asthma. (*A*) Representative Western blot depicting expression of INPP4A in the total lung lysates of human control subjects and patients with asthma, and (*B*) the densitometric quantification; $n = 6$ normal subjects, $n = 7$ patients with asthma. Results are expressed as the mean ± SEM. ***$P < 0.001$ (unpaired Student's *t* test). (*C* and *D*) INPP4A expression in BAL fluid (*C*) and sera samples (*D*) from normal human subjects and patients with asthma, determined by ELISA. Sera samples: $n = 22$ normal subjects, $n = 27$ patients with asthma; BAL fluid samples: $n = 3$ normal subjects and $n = 3$ patients with asthma. (*E*) Expression of INPP4A in the BAL fluid of mice with (ovalbumin [OVA]/OVA; $n = 5$) and without (sham/PBS; $n = 4$) allergic airway inflammation (AAI). (*C–E*) Results are expressed as the mean ± SEM. *$P < 0.05$, **$P <$ 0.01, and ***$P < 0.001$. For analysis of INPP4A in physiological fluids, statistical differences were calculated using a one-tailed Student's *t* test in the direction of human total lung lysate data.

with anti-INPP4A antibody. However, we observed marked collagen deposition in the subepithelial region upon neutralization of secretory INPP4A (Figure 2F). To further evaluate the extent of subepithelial fibrosis in the naive mice, we assessed the expression of α-SMA and found it to be increased in the lung mesenchyme (Figure 2G). We also assessed fibroblast hyperplasia, by measuring the level of

Ki-67, a marker of cellular proliferation. Colocalization of Ki-67 with α-SMA indicated hyperproliferation of lung myofibroblasts upon treatment of the mice with anti-INPP4A antibody (Figures 2H and E1E). We also found the soluble collagen content to be significantly increased in the lungs of mice treated with anti-INPP4A antibody as compared with the isotype controls (Figure 2I). Given the

known role of INPP4A as an inhibitor of the PI3K/Akt pathway, we checked the levels of phosphorylated Akt (pAkt) in the lungs and found them to be increased in the anti-INPP4A–treated samples (Figure 2J; quantified in Figure 2K).

Treatment with Anti-INPP4A Antibody Aggravates Airway Inflammation and Remodeling in a Murine Model of AAI

To determine the pathophysiological relevance of extracellular INPP4A, we repeated the antibody neutralization of extracellular INPP4A in an experimental model of AAI (Figure 3A). Neutralization of extracellular INPP4A was confirmed by assessing INPP4A activity in the BALF of mice (Figure E2A). Treatment of the mice with anti-INPP4A antibody led to increased AHR (Figure 3B) and increased airway inflammation (Figure 3C; quantified in Figure E2B). We observed an increase in the total leukocyte count in the BALF (Figure E2C). The differential leukocyte counts in the BALF revealed a significant increase in the number of eosinophils after treatment with anti-INPP4A antibody (Figure E2D). There was a concomitant increase in goblet-cell metaplasia (Figure 3D) and subepithelial fibrosis (Figure 3E). Increased expression of α-SMA and its colocalization with Ki-67 revealed lung myofibroblast hyperproliferation in mice treated with anti-INPP4A antibody (Figures 3F and E2E). The soluble collagen content was also significantly increased upon anti-INPP4A antibody treatment (Figure 3G). This was associated with an increase in T-helper cell type 2 inflammatory cytokines such as IL-4, IL-5, and IL-13 in the total lung lysates (Figures E3A–E3C). OVA-specific IgE and IgG1 were also elevated in the sera samples of mice treated with anti-INPP4A antibody (Figures E3D and E3E). To check the status of PI3K/Akt signaling, we determined key indicators of this pathway in lung tissue. We found that anti-INPP4A treatment in mice with AAI led to overactivation of PI3K/Akt signaling, as seen by the increased expression of PDK1 (Figure 3H), pAkt serine, and pAkt threonine (Figures 3I and 3J).

Enzymatically Active INPP4A Is Secreted in Cell Culture–Conditioned Media

Prior experiments had confirmed that extracellular INPP4A is functionally important *in vivo* and is secreted at high

Figure 2. Antibody-mediated neutralization of INPP4A in naive mice leads to induction of an asthma-like phenotype. (*A*) Experimental protocol for antibody-mediated neutralization of INPP4A in naive mice. AHR = airway hyperresponsiveness; i.p. = intraperitoneal. (*B*) Total airway resistance upon methacholine challenge after treatment with anti-INPP4A or isotype antibody in naive mice. Ab = antibody. (*C*) Correlation analysis of INPP4A activity in BAL fluid with % baseline total airway resistance of mice treated with isotype or anti-INPP4A antibody. OD_{450} = optical density 450. (*D–F*) Histopathological analysis of lung sections of mice to assess airway inflammation by hematoxylin and eosin (H&E) staining (*D*), goblet cell metaplasia by periodic acid–Schiff

levels in normal mice. We previously reported that INPP4A is predominantly present in the bronchial epithelial cells of the lung (6); therefore, to determine whether airway epithelium secretes INPP4A and to understand the mechanism of epithelial secretion of INPP4A in the present work, we used cultured BEAS-2B cells. Conditioned media from the cells was concentrated using either trichloroacetic acid–based precipitation or 100 kD cutoff centrifugal filters. We found that extracellular INPP4A was enzymatically active, as shown by positive INPP4 lipid phosphatase activity in the conditioned media of the cells (Figure 4A). The presence of secretory INPP4A was also shown by immunoblotting in conditioned media of BEAS-2B cells (Figure 4B; other representative blots in Figure E4). Additionally, we confirmed the secretion of INPP4A in the conditioned media of primary normal human bronchial epithelial cells (Figure 4C).

INPP4A Is Secreted via Unconventional Mechanisms into the Membrane of Vesicles and as a Free, Nonvesicle-Bound Form

After validating the extracellular presence of INPP4A, we investigated the mode of secretion of INPP4A from the cell. Through an *in silico* prediction analysis (29), we found that none of the isoforms of INPP4A had a signal peptide to drive it through the classical secretory pathway (data not shown). However, there are several proteins that are secreted despite the absence of any leader peptide (13–15). One of the important modes of such an unconventional secretion is via EVs. Interestingly, INPP4A is known to localize to endosomes (9, 10), which are primary organelles involved in exosome biogenesis. In our study also, we found that INPP4A was colocalizing with RAB5, an early endosome marker (Figure 5A; quantified in Figure 5D). To further understand the mechanism of INPP4A secretion, we

colocalized INPP4A with RAB27A and RAB27B, which are well-known regulators of vesicular exocytosis (30–32) (Figures 5B and 5C). We found that INPP4A was strongly colocalized with RAB27B (quantified in Figure 5D). To gain more insight into this colocalization, we also plotted scatter plots and line profiles for RAB5-INPP4A, RAB27A-INPP4A, and RAB27B-INPP4A images using Leica LAS AF software (Figures E5A–E5C). In a scatter plot, the two fluorescence intensity values for each pixel are plotted against each other, whereas a line profile plots modulations in the fluorescence intensities of two proteins along a defined region of interest. A synchronous rise and fall in the fluorescence intensities of RAB27B and INPP4A at multiple regions of interest confirmed colocalization of the two proteins. This indicates vesicular exocytosis as a mechanism of secretion of INPP4A (Figure E5C). To check the secretion of INPP4A in EVs, we isolated them from the cell culture medium of BEAS-2B cells using differential ultracentrifugation. We found that INPP4A could be recovered from 10K (microvesicle) and 100K (exosome) fractions, although at variable levels (Figure 5E). Heat shock protein 70 (HSP70) and tumor susceptibility gene 101 (TSG101) were used as markers of EVs. HSP70 has been shown to be present in multiple EVs, and TSG101 is enriched in lighter, small EVs (33). Apart from the EV fractions, we also checked the presence of INPP4A in a portion of the supernatant obtained after pelleting exosomes (the post-100K fraction) (Figure 5E). Detection of INPP4A in this post-100K fraction indicates secretion of a nonvesicle-bound, free form of INPP4A, along with a vesicular secretory form. The mechanism of this EV-free secretion of INPP4A, however, remains to be explored.

To better understand the EV biology of INPP4A, we used the MCF-7 cell line (breast cancer epithelial cell line) because it is easy to culture, which makes it easier to isolate

abundant amounts of exosomes. We characterized the size and morphology of exosomes by using transmission electron microscopy, which showed vesicles with a lipid bilayer and within the designated size range of 50–100 nm, conforming with the reported exosome morphology (19) (Figure E6A). Similar to what was found for the BEAS-2B cells, in MCF-7 cells INPP4A was observed in microvesicles, exosomes, and the EV-free fraction (Figure E6B). We observed a similar trend of INPP4A being present in EVs in serum-supplemented conditioned medium as well (Figure E6C).

Additionally, to perform an in-depth characterization of INPP4A in the exosomal fraction and ensure that protein aggregates were not pelleting down upon ultracentrifugation, we performed an Optiprep-based density gradient centrifugation of the 100K (exosomal) pellet (Figure E6D). We found that INPP4A was present in higher-density exosomes along with HSP70 and in lighter exosomes enriched in HSP70 and TSG101. We next examined the localization of INPP4A in exosomes by carrying out a protease protection assay. Exosomes isolated by differential centrifugation were treated with Proteinase K alone or in combination with detergent Triton X-100 (Figure E6E). We found that INPP4A was degraded by the protease treatment, even in the absence of a detergent, indicating the presence of INPP4A on the outer leaflet of the exosomes. CD63, being a transmembrane protein, showed a partial degradation upon addition of protease alone.

Altogether, our data show an unconventional secretion of INPP4A from epithelial cells, in EVs as well as in a nonvesicular free form.

Extracellular INPP4 Mediates Epithelial–Fibroblast Communication in the Lung and Controls Proliferation in the Recipient Cells

Because the communication between epithelial cells and fibroblasts is critical for

---

Figure 2. (Continued). (PAS) staining (*E*), and subepithelial fibrosis by Masson's trichrome (MT) staining (*F*). Scale bar: 100 μm. (*G*) Immunohistochemistry (IHC) to assess the expression of α-smooth muscle actin (α-SMA) in lung sections. Brown color indicates positive expression of α-SMA; nuclei are stained in blue color. Scale bar: 100 μm. (*H*) Immunofluorescence (IF) with anti-Ki67 (red) and anti–α-SMA (green) in lung sections of naive mice treated with isotype or anti-INPP4A antibody (panel elaborated, along with isotype-matched control IgG, in Figure E1E). Nuclei are stained by DAPI (blue). Br = bronchus. Scale bar: 100 μm. (*I*) Content of soluble collagen in the lungs of mice treated with isotype or anti-INPP4A antibody as measured by Sircol assay. (*J* and *K*) Immunoblotting for expression of pAkt with respect to total Akt in the lung samples of antibody-treated mice (*J*), and its densitometric analysis (*K*). Results are expressed as the mean ± SEM (*n* = 3–10 mice/group). *$P < 0.05$ and ***$P < 0.001$ versus isotype antibody. Statistical differences were calculated in the naive mouse model experiment using Student's *t* test.
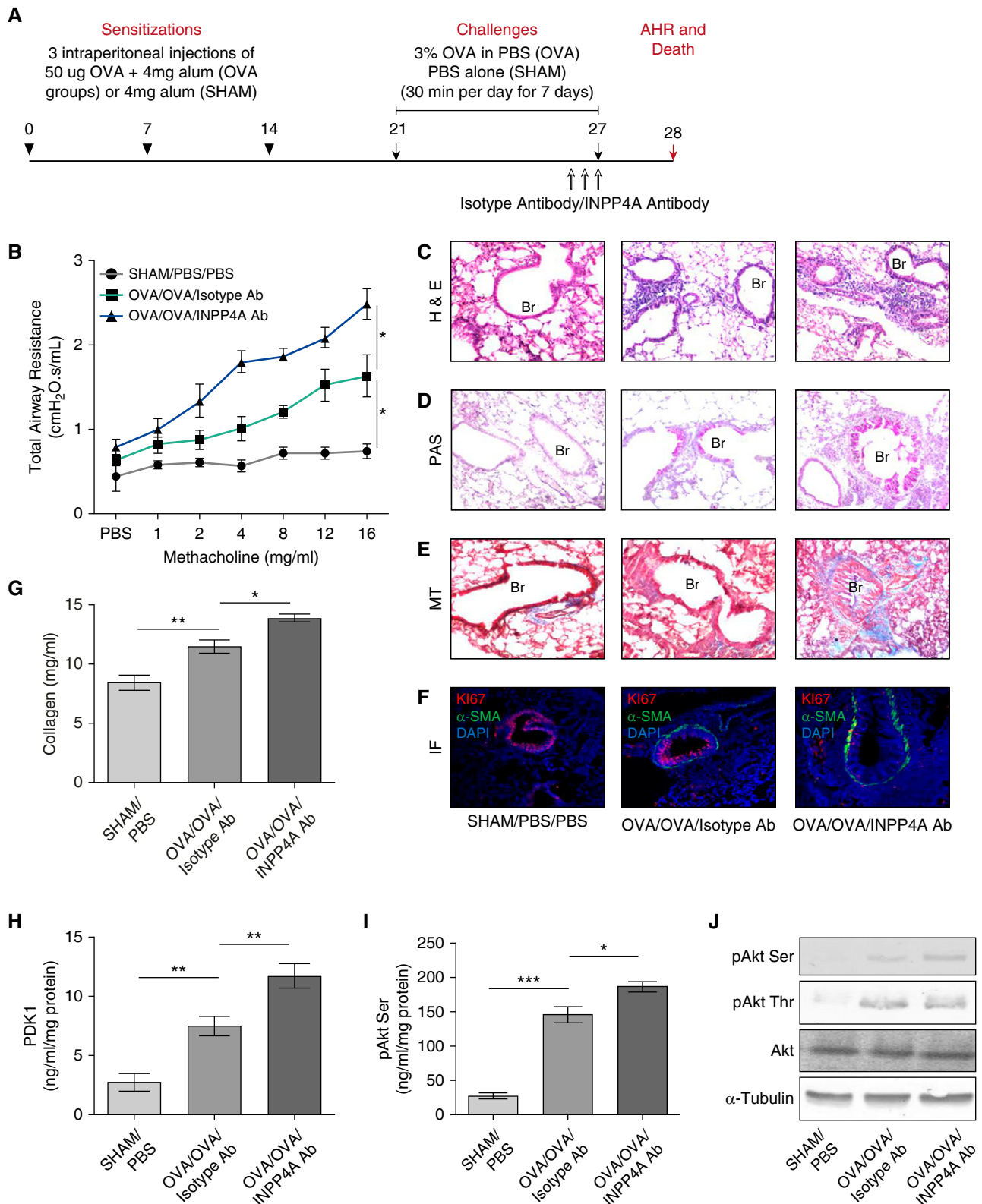
Figure 3. Treatment with anti-INPP4A antibody aggravates airway inflammation and remodeling in a murine model of AAI. (*A*) Experimental protocol of antibody-mediated neutralization of INPP4A in a murine model of AAI, developed using sensitization with intraperitoneal injections of 50 μg OVA followed by challenges with 3% aerosolized OVA. (*B*) Total airway resistance upon methacholine challenge in mice without AAI (sham) and allergic mice (OVA) treated with isotype antibody or anti-INPP4A antibody. (*C*) Airway inflammation upon antibody treatment as seen by H&E staining. (*D*) Goblet cell
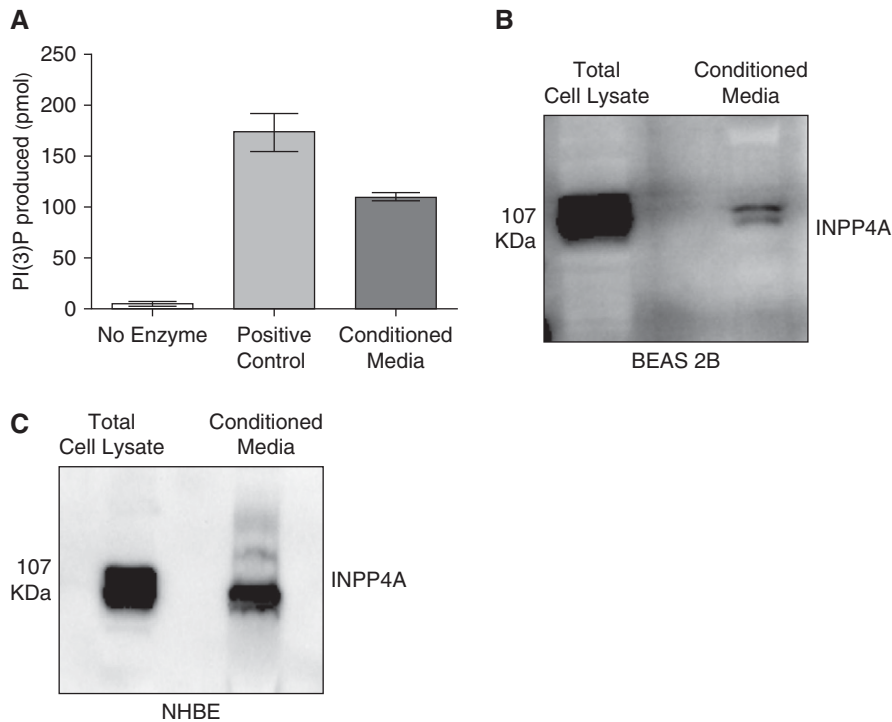
Figure 4. Enzymatically active INPP4A is secreted in cell culture–conditioned media. (*A*) INPP4 activity, depicted by the amount of phosphatidyl inositol 3-phosphate (PI[3]P) produced, in the conditioned media of bronchial epithelial cells (BEAS-2B) as measured by competitive ELISA. Results are expressed as the mean ± SEM (*n* = 4). (*B* and *C*) Representative Western blot of INPP4A expression and secretion in the cell lysate and conditioned media of BEAS-2B cells (*B*) and primary normal human bronchial epithelial (NHBE) cells (*C*). Readers may view the uncut gels for *B* in the data supplement.

maintaining lung homeostasis, and our *in vivo* data highlight the hyperproliferative phenotype in the fibroblasts upon neutralization of secretory INPP4A (as described in Figure 2), we sought to determine the role of extracellular INPP4A in facilitating such an epithelium–fibroblast crosstalk. We found that both intracellular (Figure 6A) and extracellular (Figure 6B) levels of INPP4A were higher in the human lung epithelial cells (BEAS-2B) as compared with human lung fibroblasts (MRC-5 and HFL cells). INPP4 activity was also higher in the conditioned media of the epithelial cells relative to the fibroblast cells (Figure 6C). This observation and previous reports describing lung epithelial cells as the main source of EVs in the lung (24, 26)

led us to hypothesize that INPP4A secreted from the epithelial cells could be taken up by the fibroblast cells and consequently keep a check on the proliferation of the fibroblast cells. To assess the uptake of INPP4A, we created a cell line that stably expresses GFP-tagged INPP4A in MCF-7 (MCF-ST; MCF-7 cells used for the ease of transfection). We confirmed that MCF-ST cells were secreting GFP-tagged INPP4A, as seen by immunoblotting in the conditioned medium of MCF-ST cells (Figure E7A). To ascertain whether this secreted INPP4A-GFP could be taken up by other cells, we performed a conditioned medium transfer experiment between MCF-ST and untransfected MCF-7 cells. The total cell lysate of untransfected MCF-7

showed the presence of INPP4A-GFP when incubated with conditioned medium of MCF-ST, illustrating the uptake (Figure E7B). INPP4A-GFP was also found to be released in EVs isolated from the conditioned medium of MCF-ST cells upon differential ultracentrifugation (Figure E7C). Next, the exosomes isolated from MCF-7 ST were loaded onto lung fibroblasts and immunocytochemistry was used to probe for GFP in these recipients (Figure 6D). We observed uptake of GFP-tagged INPP4A by the recipients after 3 hours of loading with INPP4A-GFP exosomes (Figure 6Ei). An enrichment of GFP at the cell membrane was observed, as shown by the orthogonally sliced image (Figure 6Eii). Because INPP4A negatively regulates the PI3K pathway by acting at the cell membrane, we hypothesized that extracellular INPP4A entering the recipient cells could be regulating cellular proliferation in them. To examine this issue, we performed an *in vitro* adaptation of the *in vivo* neutralization experiment. The cell culture medium from lung epithelial cells (BEAS-2B) was incubated with anti-INPP4A antibody or isotype IgG control for 24 hours, and then the conditioned media was transferred onto lung fibroblast cells (MRC-5) and checked for proliferation of MRC-5 using a CFSE dye dilution assay (34) (Figure 6F). The time taken by CFSE to dilute to half the fluorescent intensity ($t_{1/2}$) is inversely proportional to the extent of cellular proliferation. The $t_{1/2}$ of cultured fibroblasts, treated with control isotype antibody, was almost double that of the post–epithelial-conditioned-media transfer (30.46 ± 1.141 vs. 56.72 ± 3.868 h; $P < 0.001$; Figure 6G, I vs. II), confirming that epithelial cells were secreting products that inhibit fibroblast proliferation. Preincubation of epithelial-conditioned media with anti-INPP4A eliminated most of its antiproliferative effect on fibroblasts ($t_{1/2} = 38.31 ± 2.548$ h; Figure 6G, III). Anti-INPP4A had no direct effect on fibroblast proliferation in the absence of epithelial-conditioned

Figure 3. (Continued). metaplasia as seen by PAS staining. (*E*) Subepithelial fibrosis as seen by MT staining in lung sections. (*F*) Representative confocal fluorescence images showing α-SMA (green) and proliferation marker Ki67 (red) in the lung sections of mice treated with isotype or anti-INPP4A antibody (panel elaborated, along with isotype-matched control IgG, in Figure E2E). Nuclei were detected with DAPI (blue). (*G*) Content of soluble collagen in the lung samples as measured by Sircol assay. (*H* and *I*) Expression levels of phosphoinositide-dependent kinase-1 (PDK1) (*H*) and pAkt Ser in the total lung protein using ELISA (*I*). (*J*) Immunoblotting in the lung samples for the expression of pAkt Ser and pAkt Thr with respect to total Akt and α-tubulin. Results are expressed as the mean ± SEM (*n* = 3–6 mice/group). *$P < 0.05$, **$P < 0.01$, and ***$P < 0.001$ (ANOVA followed by Tukey's *post hoc* analysis).
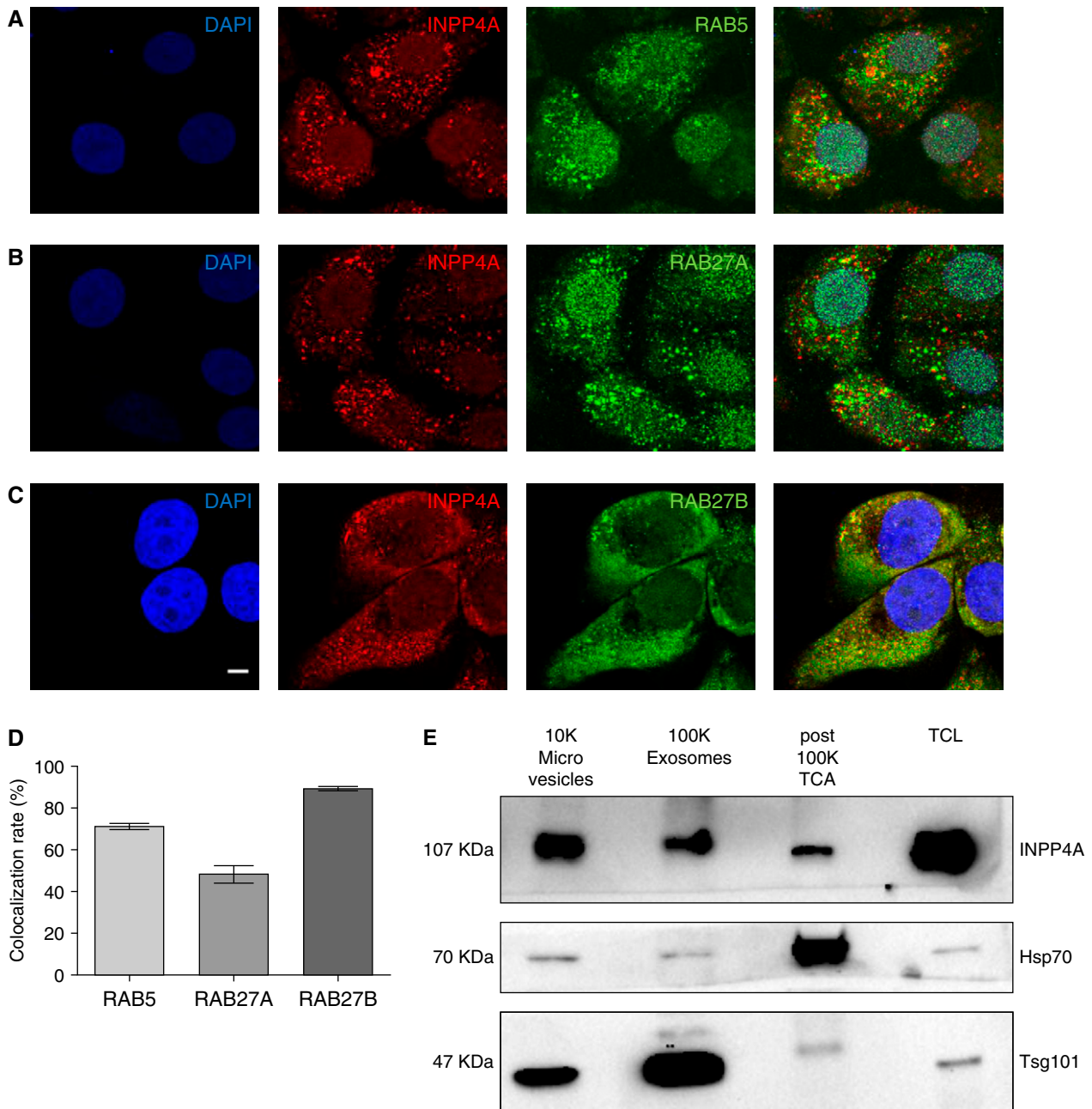
Figure 5. INPP4A is secreted via unconventional mechanisms into the membrane of extracellular vesicles (EVs) and as a free, nonvesicle-bound form. (*A–C*) Representative confocal fluorescence images of BEAS-2B cells costained with INPP4A (red) and endosome marker RAB5, or with RABs involved in vesicular exocytosis (RAB27A and RAB27B) (green). Nuclei are stained by DAPI (blue). Scale bar: 5 μm. (*D*) Bar plot showing mean colocalization rate of INPP4A with the three RABs as calculated by an automated module in Leica LAS AF software. This value indicates the extent of colocalization in percentage. Colocalization rate (%) = area colocalization/area foreground; area foreground = area image − area background. (*E*) Representative immunoblot of the INPP4A and EV markers tumor susceptibility gene 101 (TSG101) and heat shock protein 70 (HSP70) in the EV fractions isolated by differential ultracentrifugation of the conditioned media of BEAS-2B cells. 10K = 10,000 × *g* pellet (microvesicles); 100K = 100,000 × *g* pellet (exosomes). TCL = total cell lysate. INPP4A was also detected in the EV-free fraction, as seen in the trichloroacetic acid (TCA) precipitate of a portion of the supernatant obtained after the 100,000 × *g* centrifugation (post-100k TCA fraction). Results are expressed as the mean ± SEM.

media transfer (30.46 ± 1.141 vs. 26.98 ± 1.139, *P* = not significant; Figure 6G, I vs. IV). We observed a similar trend when the BEAS2B-conditioned media was

transferred onto primary normal human lung fibroblasts (Figure 6H). The proliferation of primary fibroblasts was inhibited when they were cultured in the

presence of epithelial cell–conditioned media. Similar to what was observed with the MRC-5 cells, anti-INPP4A antibody pretreatment of the epithelial conditioned
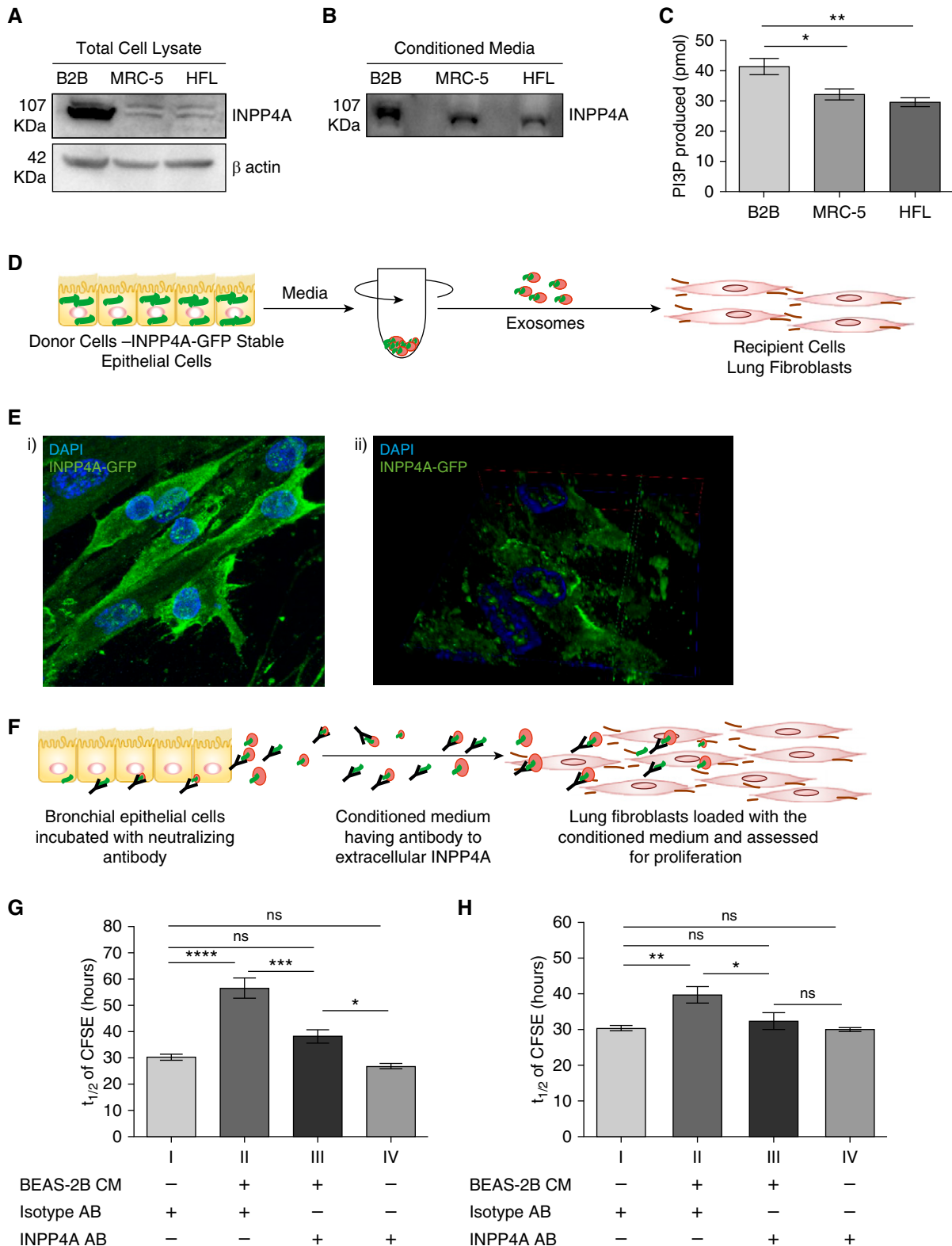
Figure 6. Extracellular INPP4A mediates epithelial–fibroblast communication in the lung and controls proliferation in the recipient cells. (*A*) Representative immunoblot of INPP4A in lysates of BEAS-2B cells (represented as B2B) and lung fibroblasts (MRC-5 and human lung fibroblast [HFL] cells). (*B*) Representative immunoblot of INPP4A in the conditioned media of the cells. Normalization by equal seeding density as elaborated in METHODS. (*C*) INPP4 activity in the cell-conditioned media; $n = 3–7$ per group. (*D*) Schematic diagram showing isolation of exosomes from MCF-ST cells by differential ultracentrifugation and loading onto MRC-5. (*Ei*) Representative fluorescent image of MRC-5 cells loaded with exosomes isolated from MCF-ST and

media decreased the antiproliferative effect on primary fibroblasts.

Overall, this was consistent with the model that epithelial cells secrete INPP4A, which is taken up by fibroblasts, retarding their proliferation and thus mediating an epithelial–fibroblast crosstalk.

Discussion

Previous studies from our lab, at both genetic and functional levels, have shown a critical role for INPP4A in asthma. Here, we add a novel layer to the INPP4A–asthma link, showing for the first time that INPP4A is secreted extracellularly, where it suppresses AAI and remodeling. We provide a plausible mechanism, showing that cultured airway epithelial cells secrete INPP4A-containing EVs, which in turn can be taken up by fibroblasts, thus limiting their proliferative capacity. Although we have not determined the source of extracellular INPP4A *in vivo*, it is likely to be the airway epithelial cells, for the following reasons: first, we have previously shown that INPP4A expression is maximally seen in the airway epithelium (6); second, the epithelium is known to be a major secretor of EVs in the lung (24, 26); and third, the pattern of extracellular INPP4A tracks that of airway epithelial expression of INPP4A. In asthma, where EV-producing inflammatory cells are increased, extracellular INPP4A is decreased. In the current study, we report that INPP4A is secreted by bronchial epithelial cells in EVs as well as in a free form. Damage to the lung epithelium, as seen in asthma and other respiratory diseases (35–38), can thus decrease the level of secretory INPP4A. This loss of secretory INPP4A translates to a loss of the braking mechanism and can lead to unrestrained proliferation of the fibroblasts, ultimately resulting in airway remodeling (Figure 7).

Our finding adds to a growing list of proteins that were previously thought to be intracellular but are now also found to be released extracellularly. Another negative regulator of the PI3K signaling, PTEN, has also been shown to be secreted in exosomes. Exosomal PTEN can be taken up by other cells, reduce the levels of pAkt in the recipients, and thereby downregulate cellular proliferation in them (39). Proteins that can dampen the JAK STAT pathway, SOCS1 and SOCS3, were also recently shown to get secreted in microvesicles and exosomes (22). Alveolar macrophages constitutively secrete these SOCS proteins, which upon being taken up by the alveolar epithelial cells lead to inhibition of cytokine-induced STAT signaling within the recipients. These dual roles of critical signaling proteins suggest intricately connected intracellular and intercellular effects that may be required to maintain lung structure and function.

One of the possibilities that we explicitly eliminated was that INPP4A may be getting released nonspecifically. First, we demonstrated the secretion of INPP4A in EVs, including exosomes. It is now strongly established that sorting of cargo to these EVs is a selective, rather than random, process. Colocalization of INPP4A to the RABs involved in vesicular exocytosis also indicates a regulated secretion of INPP4A. Second, and possibly most importantly, antibody-mediated neutralization of extracellular INPP4A had notable effects *in vitro* and *in vivo*, confirming its functional importance. Neutralizing secretory INPP4A in the conditioned media of bronchial epithelial cells and incubating it with lung fibroblasts increased proliferation of the fibroblasts. Treating naive mice with INPP4A-neutralizing antibody increased fibroblast proliferation and led to substantial collagen deposition and elevated AHR. Neutralizing INPP4A in allergic mice aggravated the asthma features.

The precise mechanisms of INPP4A secretion and the potentially different roles of differently secreted forms remain unclear. In the present study, we demonstrated the release of INPP4A in various EVs as well as in a free, nonvesicular form. Vesicle-bound forms have the advantage of being transported to remote destinations in the body without being degraded. Exosomes derived from tumor cells have been shown to carry cargo to distant sites and convert them into premetastatic niches (40, 41). The nonvesicle form, however, can mediate effects within neighboring tissue spaces only. It is interesting to note that INPP4A uses both of these modes for secretion. However, which form is more efficient in mediating the downstream proliferation effect in recipient cells remains to be determined. We speculate that the EV-bound form may be more effective due to its membrane-enriched delivery. The mechanism of secretion of the free form of INPP4A is unknown. INPP4A could be directly secreted from the cell through membrane transporters. It could also be present in secretory lysosomes and get released outside the cells upon fusion of these specialized lysosomes with the plasma membrane. Colocalization of INPP4A with RAB27A, which mediates the transport of secretory lysosome to the plasma membrane, is consistent with this path (42). Along with the mechanism of secretion, the modulators of secretion are also relevant. Our study shows that allergic conditions lead to decreased levels of secretory INPP4A; however, what specific biological factors are responsible for modulating the secretion remains to be explored. Another interesting aspect of this study is the localization of INPP4A to the outer leaflet of exosomes. This is quite intriguing, as INPP4A is a leaderless protein and associates with the outer membrane of endosomes. These observations point to a lumenal localization of INPP4A in the exosomes; though, the protease protection assay in our study indicates presence of

Figure 6. (Continued). imaged after 3 hours. Nuclei are stained by DAPI (blue). (*Eii*) A three-dimensionally rotated and orthogonally sliced representation of the fluorescence image shows prominent membrane localization of INPP4A-GFP in the recipient MRC-5 cells. (*F*) Schematic diagram illustrating the incubation of BEAS-2B with antibody for neutralizing secretory INPP4A and loading of this conditioned medium (CM) on lung fibroblasts, followed by checking recipient cell proliferation. (*G* and *H*) Half-life of fluorescence intensity of carboxyfluorescein diacetate succinimidyl ester (CFSE) ($t_{1/2}$) in labeled lung fibroblasts (MRC-5 cells [*G*] and primary normal human lung fibroblasts [*H*]) upon treatment of the fibroblast medium directly with isotype or anti-INPP4A antibody, or when fibroblasts were cultured in conditioned media derived from bronchial epithelial cells, with or without neutralization of extracellular INPP4A ($n = 5$ [*G* and *H*]). The half-life of CFSE was measured by monitoring the decrease in CFSE intensity with respect to the harvest time using flow cytometry. Anti-INPP4A antibody used to neutralize extracellular INPP4A; isotype antibody served as the control. Results are expressed as the mean ± SEM. *$P < 0.05$, **$P < 0.01$, ***$P < 0.001$, and ****$P < 0.0001$; ns = not significant (ANOVA followed by Tukey's *post hoc* analysis).

Normal Airways

Allergic Airways

↑ **Extracellular INPP4A**

↓ **Extracellular INPP4A**

Normal Fibroblast Proliferation

Fibroblast Hyperproliferation

Healthy Epithelium **Damaged Epithelium** **Fibroblast Cells** **Extracellular Vesicles** **INPP4A**
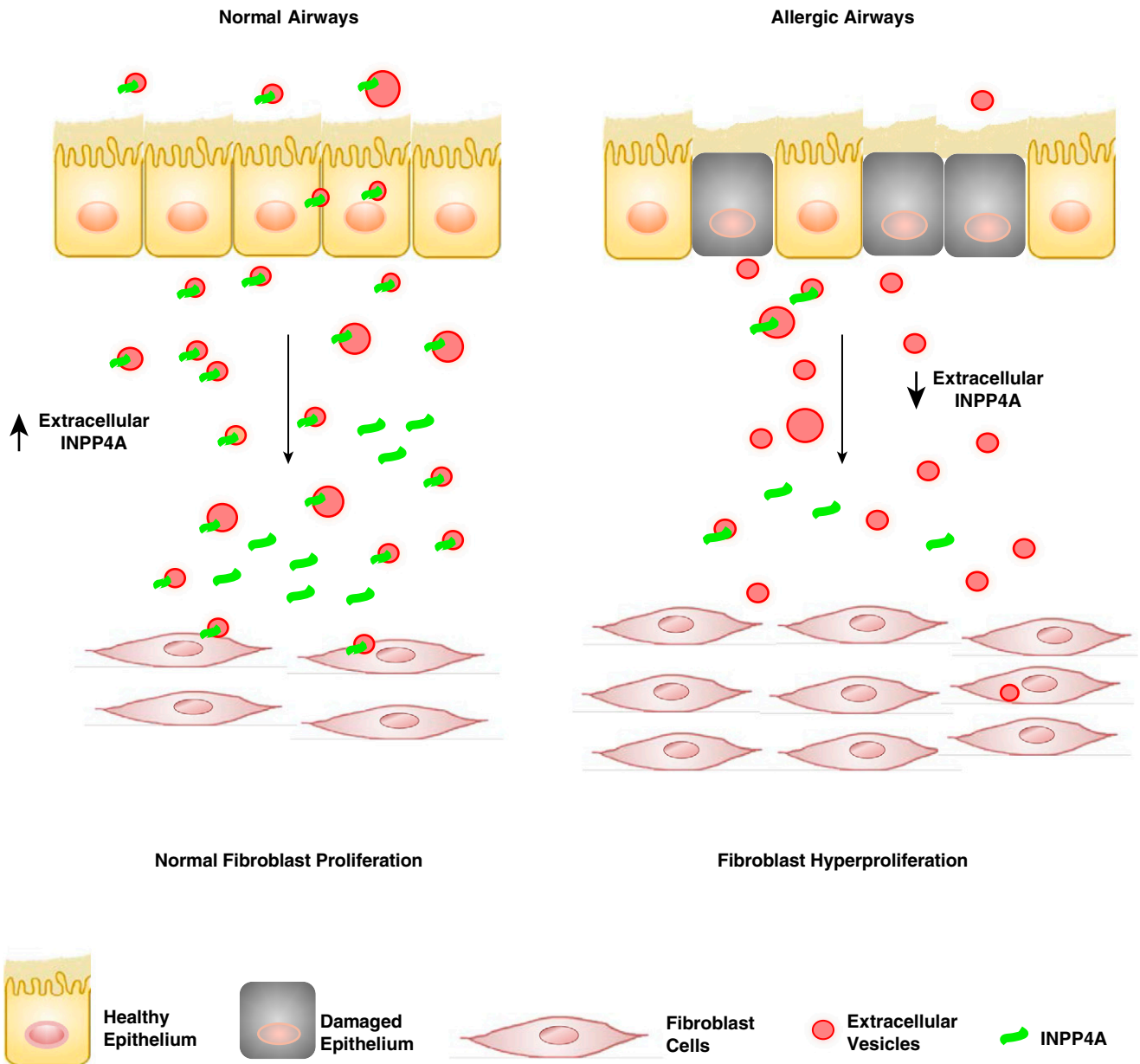
Figure 7. Schematic model depicting the potential role of extracellular INPP4A. In normal airway physiology, extracellular INPP4A transferred from epithelial cells to fibroblasts reduces the proliferation of the latter, highlighting the role of extracellular INPP4A in maintaining a check on fibroblast growth. In allergic airways, damaged epithelium and a concomitant decrease in extracellular INPP4A may eliminate this control and lead to fibroblast hyperproliferation and airway remodeling, a key feature of asthma pathophysiology.

INPP4A to the outer leaflet of exosomes. Another leaderless exosomal protein, Annexin A2 also shows both lumenal and surface localization on exosomes (43). The pathway taken by both of these proteins to localize to the surface of exosomes is currently unclear. In-depth studies of the trafficking of such proteins could shed light on any unconventional protein trafficking pathway mediating such "inside-out" localization.

Because our previous study showed predominant localization of INPP4A in bronchial epithelial cells, in this work we focused on secretion of INPP4A from this cell type in the lungs. However, other cell types, such as endothelial cells, alveolar macrophages, platelets, and immune cells, are also important in pulmonary EV biology, and thus secretion of INPP4A from these cell types (if it occurs) could also help maintain lung homeostasis.

Although INPP4A is believed to act via the PI3K/Akt pathway, and we observed changes consistent with that model in our study, a recent study from our lab additionally indicated a novel, non–PI3K-dependent role of INPP4A in inhibiting cellular proliferation (44). This has not yet been explored in the context of asthma pathogenesis, but it merits further research.

A previous genetic study from our lab showed that a nonsynonymous SNP in

INPP4A, which decreased the stability of the protein in platelets obtained from human subjects, was associated with atopic asthma (5). Our follow-up report detailing the functional role of INPP4A in allergic asthma showed that overexpression of INPP4A in a murine model of acute airway inflammation led to the alleviation of asthma features (6, 45). These studies highlight the protective effect of INPP4A in asthma, and suggest that increasing the levels of INPP4A can provide marked benefits in restoring pulmonary homeostasis.

In the current study, we observed aggravation of asthma phenotypes upon neutralization of extracellular INPP4A, which underlines the importance of extracellular INPP4A in maintaining lung physiology. Because increasing intracellular INPP4A levels by specific cellular deliveries is nontrivial, the alternate approach of increasing extracellular INPP4A seems to be promising. With implications for health and disease, EVs offer new targets for therapeutic interventions (46, 47). Loading EVs with INPP4A and delivering them to

the lungs of patients showing loss of INPP4A could be a novel therapeutic strategy. ■

References

1. Norris FA, Majerus PW. Hydrolysis of phosphatidylinositol 3,4-bisphosphate by inositol polyphosphate 4-phosphatase isolated by affinity elution chromatography. *J Biol Chem* 1994;269:8716–8720.
2. Norris FA, Atkins RC, Majerus PW. Inositol polyphosphate 4-phosphatase is inactivated by calpain-mediated proteolysis in stimulated human platelets. *J Biol Chem* 1997;272:10987–10989.
3. Munday AD, Norris FA, Caldwell KK, Brown S, Majerus PW, Mitchell CA. The inositol polyphosphate 4-phosphatase forms a complex with phosphatidylinositol 3-kinase in human platelet cytosol. *Proc Natl Acad Sci USA* 1999;96:3640–3645.
4. Ivetac I, Gurung R, Hakim S, Horan KA, Sheffield DA, Binge LC, et al. Regulation of PI(3)K/Akt signalling and cellular transformation by inositol polyphosphate 4-phosphatase-1. *EMBO Rep* 2009;10:487–493.
5. Sharma M, Batra J, Mabalirajan U, Sharma S, Nagarkatti R, Aich J, et al. A genetic variation in inositol polyphosphate 4 phosphatase a enhances susceptibility to asthma. *Am J Respir Crit Care Med* 2008; 177:712–719.
6. Aich J, Mabalirajan U, Ahmad T, Agrawal A, Ghosh B. Loss-of-function of inositol polyphosphate-4-phosphatase reversibly increases the severity of allergic airway inflammation. *Nat Commun* 2012;3:877.
7. Vyas P, Norris FA, Joseph R, Majerus PW, Orkin SH. Inositol polyphosphate 4-phosphatase type I regulates cell growth downstream of transcription factor GATA-1. *Proc Natl Acad Sci USA* 2000;97: 13696–13701.
8. Wang C, Feng Z, Jiang K, Zuo X. Upregulation of microRNA-935 promotes the malignant behaviors of pancreatic carcinoma PANC-1 cells via targeting inositol polyphosphate 4-phosphatase type I gene (INPP4A). *Oncol Res* 2017;25:559–569.
9. Ivetac I, Munday AD, Kisseleva MV, Zhang X-M, Luff S, Tiganis T, et al. The type Ialpha inositol polyphosphate 4-phosphatase generates and terminates phosphoinositide 3-kinase signals on endosomes and the plasma membrane. *Mol Biol Cell* 2005;16:2218–2233.
10. Shin HW, Hayashi M, Christoforidis S, Lacas-Gervais S, Hoepfner S, Wenk MR, et al. An enzymatic cascade of Rab5 effectors regulates phosphoinositide turnover in the endocytic pathway. *J Cell Biol* 2005;170:607–618.
11. Osborne AR, Rapoport TA, van den Berg B. Protein translocation by the Sec61/SecY channel. *Annu Rev Cell Dev Biol* 2005;21:529–550.
12. Lee MCS, Miller EA, Goldberg J, Orci L, Schekman R. Bi-directional protein transport between the ER and Golgi. *Annu Rev Cell Dev Biol* 2004;20:87–123.
13. Nickel W, Rabouille C. Mechanisms of regulated unconventional protein secretion. *Nat Rev Mol Cell Biol* 2009;10:148–155.
14. Zhang M, Schekman R. Cell Biology. Unconventional secretion, unconventional solutions. *Science* 2013;340:559–561.
15. Rabouille C. Pathways of unconventional protein secretion. *Trends Cell Biol* 2017;27:230–240.
16. Zehe C, Engling A, Wegehingel S, Schäfer T, Nickel W. Cell-surface heparan sulfate proteoglycans are essential components of the unconventional export machinery of FGF-2. *Proc Natl Acad Sci USA* 2006;103:15479–15484.
17. Temmerman K, Ebert AD, Müller HM, Sinning I, Tews I, Nickel W. A direct role for phosphatidylinositol-4,5-bisphosphate in unconventional secretion of fibroblast growth factor 2. *Traffic* 2008;9: 1204–1217.
18. Raposo G, Stoorvogel W. Extracellular vesicles: exosomes, microvesicles, and friends. *J Cell Biol* 2013;200:373–383.
19. Colombo M, Raposo G, Théry C. Biogenesis, secretion, and intercellular interactions of exosomes and other extracellular vesicles. *Annu Rev Cell Dev Biol* 2014;30:255–289.
20. Tkach M, Théry C. Communication by extracellular vesicles: where we are and where we need to go. *Cell* 2016;164:1226–1232.
21. Kesimer M, Gupta R. Physical characterization and profiling of airway epithelial derived exosomes using light scattering. *Methods* 2015;87: 59–63.
22. Bourdonnay E, Zasłona Z, Penke LRK, Speth JM, Schneider DJ, Przybranowski S, et al. Transcellular delivery of vesicular SOCS proteins from macrophages to epithelial cells blunts inflammatory signaling. *J Exp Med* 2015;212:729–742.
23. Torregrosa Paredes P, Esser J, Admyre C, Nord M, Rahman QK, Lukic A, et al. Bronchoalveolar lavage fluid exosomes contribute to cytokine and leukotriene production in allergic asthma. *Allergy* 2012;67:911–919.
24. Kulshreshtha A, Ahmad T, Agrawal A, Ghosh B. Proinflammatory role of epithelial cell-derived exosomes in allergic airway inflammation. *J Allergy Clin Immunol* 2013;131:1194–1203, 1203.e1–1203.e14.
25. Szul T, Bratcher PE, Fraser KB, Kong M, Tirouvanziam R, Ingersoll S, et al. Toll-like receptor 4 engagement mediates prolyl endopeptidase release from airway epithelia via exosomes. *Am J Respir Cell Mol Biol* 2016;54:359–369.
26. Fujita Y, Kosaka N, Araya J, Kuwano K, Ochiya T. Extracellular vesicles in lung microenvironment and pathogenesis. *Trends Mol Med* 2015; 21:533–542.
27. Fujita Y, Araya J, Ito S, Kobayashi K, Kosaka N, Yoshioka Y, et al. Suppression of autophagy by extracellular vesicles promotes myofibroblast differentiation in COPD pathogenesis. *J Extracell Vesicles* 2015;4:28388.
28. Marudamuthu AS, Shetty SK, Bhandary YP, Karandashova S, Thompson M, Sathish V, et al. Plasminogen activator inhibitor-1 suppresses profibrotic responses in fibroblasts from fibrotic lungs. *J Biol Chem* 2015;290:9428–9441.
29. Petersen TN, Brunak S, von Heijne G, Nielsen H. SignalP 4.0: discriminating signal peptides from transmembrane regions. *Nat Methods* 2011;8: 785–786.
30. Romano Regazzi. Molecular mechanisms of exocytosis. New York, NY: Springer-Verlag; 2007.
31. Ostrowski M, Carmo NB, Krumeich S, Fanget I, Raposo G, Savina A, et al. Rab27a and Rab27b control different steps of the exosome secretion pathway. *Nat Cell Biol* 2010;12:19–30; sup pp 1–13.
32. Fukuda M. Rab27 effectors, pleiotropic regulators in secretory pathways. *Traffic* 2013;14:949–963.
33. Kowal J, Arras G, Colombo M, Jouve M, Morath JP, Primdal-Bengtson B, et al. Proteomic comparison defines novel markers to characterize heterogeneous populations of extracellular vesicle subtypes. *Proc Natl Acad Sci USA* 2016;113:E968–E977.

34. Filby A, Begum J, Jalal M, Day W. Appraising the suitability of succinimidyl and lipophilic fluorescent dyes to track proliferation in non-quiescent cells by dye dilution. *Methods* 2015;82: 29–37.

35. Laitinen L, Heino M, Laitinen A. Damage of the airway epithelium and bronchial reactivity in patients with asthma. *Am Rev Respir Dis* 1985; 131:599–606.

36. Lambrecht BN, Hammad H. The airway epithelium in asthma. *Nat Med* 2012;18:684–692.

37. Thorley AJ, Tetley TD. Pulmonary epithelium, cigarette smoke, and chronic obstructive pulmonary disease. *Int J Chron Obstruct Pulmon Dis* 2007;2:409–428.

38. Morissette MC, Parent J, Milot J. Alveolar epithelial and endothelial cell apoptosis in emphysema: what we know and what we need to know. *Int J Chron Obstruct Pulmon Dis* 2009;4:19–31.

39. Putz U, Howitt J, Doan A, Goh CP, Low LH, Silke J, *et al*. The tumor suppressor PTEN is exported in exosomes and has phosphatase activity in recipient cells. *Sci Signal* 2012;5:ra70.

40. Hoshino A, Costa-Silva B, Shen T-L, Rodrigues G, Hashimoto A, Tesic Mark M, *et al*. Tumour exosome integrins determine organotropic metastasis. *Nature* 2015;527:329–335.

41. Costa-Silva B, Aiello NM, Ocean AJ, Singh S, Zhang H, Thakur BK, *et al*. Pancreatic cancer exosomes initiate pre-metastatic niche formation in the liver. *Nat Cell Biol* 2015;17:816–826.

42. Blott EJ, Griffiths GM. Secretory lysosomes. *Nat Rev Mol Cell Biol* 2002;3:122–131.

43. Stewart S, Gessler F, Pluchino S, Moreau K. Inside-out: unpredicted Annexin A2 localisation on the surface of extracellular vesicles. *Matters (Zürich)* 2016;2:e201602000015.

44. Chaudhuri R, Khanna K, Desiraju K, Pattnaik B, Vatsa D, Agrawal A, *et al*. Novel nuclear translocation of inositol polyphosphate 4-phosphatase is associated with cell cycle, proliferation and survival. *Biochim Biophys Acta* 2018;1865:1501–1514.

45. Aich J, Mabalirajan U, Ahmad T, Khanna K, Rehman R, Agrawal A, *et al*. Resveratrol attenuates experimental allergic asthma in mice by restoring inositol polyphosphate 4 phosphatase (INPP4A). *Int Immunopharmacol* 2012;14:438–443.

46. EL Andaloussi S, Mäger I, Breakefield XO, Wood MJ. Extracellular vesicles: biology and emerging therapeutic opportunities. *Nat Rev Drug Discov* 2013;12:347–357.

47. Maas SLN, Breakefield XO, Weaver AM. Extracellular vesicles: unique intercellular delivery vehicles. *Trends Cell Biol* 2017;27:172–188.